CuOeNiO/Co₃O₄ hybrid nanoplates as highly active catalyst for ammonia borane hydrolysis

Jinyun Liao [a], Yufa Feng [a], Weimin Lin [a], Xinlong Su [a], Shan Ji [b],*, Liling Li [c], Wanling Zhang [a], Bruno G. Pollet [d], Hao Li [a],**

a School of Chemistry and Materials Engineering, Huizhou University, Huizhou, 516007, China

b College of Biological, Chemical Science and Chemical Engineering, Jiaxing University, Jiaxing, 314001, China

c Department of Pharmacy, Huizhou Health Sciences Polytechnic, Huizhou, 516025, China

d Hydrogen Energy and Sonochemistry Research Group, Department of Energy and Process Engineering, Faculty of Engineering, Norwegian University of Science and Technology (NTNU), NO-7491, Trondheim, Norway

Corresponding authors
E-mail addresses:
*jishan@zjxu.edu.cn (S.Ji),
**lihao180@126.com(H.Li)

Abstract

Dehydrogenation of hydrogen-rich chemicals, such as ammonia borane (AB), is a promising way to produce hydrogen for mobile fuel cell power systems. However, the practical application has been impeded due to the high cost and scarcity of the catalysts. Herein, a low-cost and high-performing core-shell structured CuOeNiO/Co₃O₄ hybrid nanoplate catalytic material has been developed for the hydrolysis of AB. The obtained hybrid catalyst exhibits a high catalytic activity towards the hydrolysis of AB with a turnover frequency (TOF) of 79.1 mol_{H2} mol cat^1 min^1. The apparent activation energy of AB hydrolysis on CuOeNiO/Co₃O₄ is calculated to be 23.7 $kJ.mol^1$. The synergistic effect between CuOeNiO and Co₃O₄ plays an important role in the improvement of the catalytic performance. The development of this high-performing and low-cost CuOeNiO/Co₃O₄ hybrid catalytic material can make practical applications of AB hydrolysis at large-scale possible.

Introduction

Due to its high energy density (three times higher than petroleum), sustainable and "clean" features, hydrogen (H₂) is being regarded as an ideal energy source for mobile and stationary fuel cell applications [1e7]. With the rapid development of fuel cell technologies, there is a huge and increased demand for producing green hydrogen cost-effectively, efficiently and safely store it. Recently, it has been found that producing hydrogen from hydrogen-rich chemicals, such as ammonia borane (NH₃BH₃) and sodium borohydride (NaBH₄) is feasible to store it and use it for fuel cell electric vehicles (FCEV) [8e13]. For example, 4 mol of hydrogen can be produced from 1 mol of NaBH₄ with the presence of a hydrolytic catalyst. Platinum-groupmetal(PGM)catalysts,suchas Pt [14], Ru [15] and Pd [16], are usually required to catalyze such hydrolysis reactions. However, their high cost and scarcity significantly impede the practical application of producing hydrogen from hydrogen-rich compounds. Therefore, it is of great significance to develop non-PGM based catalysts as alternative hydrolysis catalytic materials.

Amongst all potential alternative materials to PGM-based hydrolytic catalysts, low-cost hydrolytic catalysts, such as CuNi [17], CuCo[18], CoeWeB [19], NieCoeP [20], and CuCoO/ graphene [21], have been developed and exhibited promising catalytic performance for the hydrolysis of NaBH₄ and NH₃BH₃. For example, Co nanoparticles decorated by Cu have been successfully synthesized by a one-step self-catalytic method. It was discovered that the obtained catalysts exhibited high catalytic performance in NH₃BH₃ hydrolysis due to the effective synergistic effect between Co and Cu

[22]. Cu_2O nanoparticles with the shape of 50-facets modified with Co_3O_4 was synthesized via a conventional impregnation method by Fukuzumi et al. under strong reductive conditions, and the obtained catalyst material showed high activity towards the hydrolysis of ammonia borane [23]. Peng et al. prepared $Cu(OH)_2/Fe(OH)_3$ nanocomposite catalysts via a onestep chemical precipitation method and found that the *as*prepared catalyst demonstrated high catalytic activity in NH_3BH_3 hydrolysis with the TOF value of 50.3 $mol_{H2}.mol.cat^1.min^1$ [24]. Lee et al. reported that $Cu_xCo_{1-x}O$ nanoparticles deposited on graphene showed an excellent TOF value of 70.0 $mol_{H2}.mol.cat^1.min^1$ with good stability [8]. Chen et al. [25] prepared CueNi nanoparticles immobilized on MCM-41 using a liquid impregnation-reduction method, exhibiting a better performance in the dehydrogenation of ammonia borane than their Cu, Ni, and CueNi counterparts. All these studies clearly show that combining different transitional metal oxides or hydroxides together is a feasible and efficient way to enhance the catalytic properties. Could the catalytic activity be further enhanced via the synergetic effect between the various non-PGM compounds via synthesizing nano-sized structures and adjusting the composite? And what is the role of each transitional metal in these non-PGM catalysts? It is indeed an interesting area for the development of low-cost highly-performing catalysts for hydrolysis.

In our previous studies, yolk-shell Co_3O_4 was synthesized and then decorated by Cu, and the obtained catalyst exhibited high catalytic activity towards the ammonia borane hydrolysis reaction [26]. In this study, a catalyst containing CuO, NiO, and Co_3O_4 was developed via a simple and low-cost method. Initially, Co_3O_4 with plate-like morphology was synthesized via a hydrothermal method, and then CuO and NiO were deposited onto Co_3O_4 to improve the catalytic performance. The *as*-prepared catalytic material exhibited a good catalytic activity towards the hydrolysis of ammonia borane with a TOF value of 79.1 mol_{H2} mol cat^1 min^1, and the ammonia borane was completely hydrolyzed within 160 s.

Experimental

Preparation of CuOeNiO/Co₃O₄ hybrid nanoplates

Analytic grade chemicals from the suppliers without any purification were used for all the experiments. Ammonia borane (97.0%) was bought from Henan Lien Chemical Engineering Products Co., LTD. $Co(NO_3)_2$ (99.0%), nickelous acetate (98.0%) and sodium citrate (99.0%) was bought from Tianjin Baishi Chemical Engineering Co., LTD. NaOH (96.0%) was bought from Taishan Yueqiao Plastics Co., LTD. Cupric acetate (99.0%) and urea (99.0%) was bought from Tianjin Yongda Chemical Reagent Co., LTD. The detailed synthetic procedure for synthesizing CuOeNiO/Co₃O₄ hybrid nanoplates is as follows: $Co(NO_3)_2$ (5 mmol), sodium citrate (10 mmol) and NaOH (100 mmol) were dissolved in 5 mL, 40 mL and 20 mL of water to form solutions A, B, and C respectively. Solution A was slowly mixed with Solution B with magnetic stirring, and then Solution C was added dropwise into it. The obtained mixture was transferred into an autoclave and heated at 160 C for 6 h. The product was filtered out, washed with water thoroughly and then dried in a vacuum oven at 60 C for 12 h. The dried powder was then heated at 450 C for 4 h and powdery Co_3O_4 was obtained. Subsequently, 0.1 g of the obtained Co_3O_4 was added into an aqueous solution (50 mL) containing cupric acetate (2 mol/L), nickelous acetate (2 mol/L) and urea (2 mol/ L) and heated at 70 C with magnetic stirring for 12 h. After that, the product was filtered out and washed with water, and then heat-treated at 450 C

for 2 h. The final product was labeled as CuOeNiO/Co₄. The illustration of the process of CuO-NiO/Co₃O₄ can be seen in Fig. 1.

Characterization

X-Ray diffraction (XRD) patterns were recorded using a PANalytical B.V. Empyrean X-ray diffractometer with CuKa radiation (l ¼ 1.5406 A). The surface morphology of the film catalyst was studied using a Carl Zeiss Ultra Plus scanning electron microscope (SEM). The

volumetric analyzer. Energy-dispersive Xray spectroscopy (EDX) measurements were carried out on a FEI Tecnai G2 F20 high-resolution transmission electron microscope (TEM) operating at 200 kV. H₂ temperatureprogrammed reduction (H₂-TPR) experiment was performed by using an automatic chemisorption analyzer (TP5080) equipped with a TCD dictator. In this process, approximately 100 mg of the sample was treated with a 50 mL min¹ stream of 10 vol% H₂ in argon from ambient temperature to 800 C at a heating temperature rate of 10 C/min.

Catalytic activity assessment

The catalytic hydrolysis of NH₃BH₃ was carried out in a threenecked glass container connected with a gas burette to measure the accumulative volume of H₂ generated during the hydrolysis reaction. Typically, 3 mmol NH₃BH₃ and 20 mmol NaOH were mixed into the reaction vessel containing 15 mL of ultrapure water, which was poured into a suspension containing 10 mg of the well-dispersed catalyst and 5 mL of ultrapure water. As soon as the catalyst came into contact with NH₃BH₃ solution, plenteous bubbles appeared
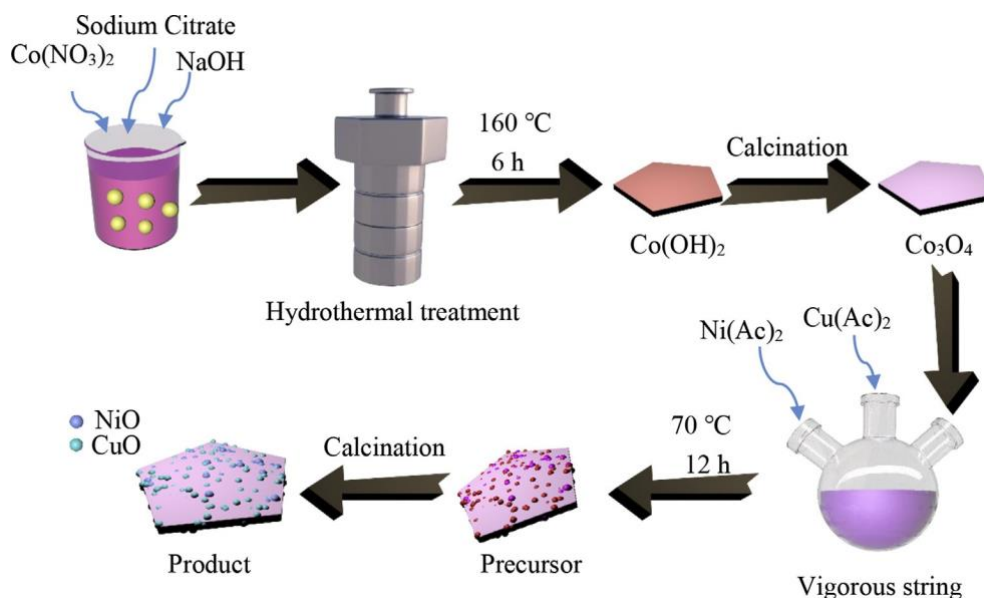

Fig. 1 e Illustration of the synthetic process of CuOeNiO/Co₃O₄.

specific surface area was determined by the Brunauer-Emmett-Teller (BET) method based upon the sorption isotherms obtained on a Quantachrome Autosorb-1

immediately, indicative of the generation of hydrogen. The reaction temperature of the hydrolytic reaction was set at 25 C using a thermostatic bath.

Results and discussion

The crystal structure of the *as*-prepared Co_3O_4 and CuOeNiO/ Co_3O_4 were investigated by XRD. As shown in Fig. 2, the XRD pattern of the Co_3O_4 exhibits all the characteristic diffraction peaks of Co_3O_4 (PDF # 42e1467) at 31.3, 36.9, 44.8, 59.4, and 65.3, corresponding to the (220), (311), (400), (511) and (440) planes, respectively. Except for the diffraction peaks of Co_3O_4, no peaks related to other forms of cobalt oxides were observed, indicating that only pure Co_3O_4 phase was formed by this method. Subsequently, CuO and NiO were depositedby reacting cupric acetate, nickelous acetate with urea and then heated at 450 C. The formation of CuO and NiO on the surface of Co_3O_4 was confirmed by the XRD pattern of CuOeNiO/ Co_3O_4, in which the X-ray diffraction peaks for CuO (PDF # 45e0937) and NiO (PDF # 47e1049) were observed. Its structure was also investigated by FT-IR. In the FT-IR spectra (Fig. 2b), theabsorptionpeak at 574and 667 cm^1 can be assigned to the Co_3O_4 spinel oxide; besides the bands for Co_3O_4, stretching bonds of CueO and NieO at 418 and 443 cm^1 respectively were

also observed, indicating that the NiO and CuO were formed on Co_3O_4 [27,28].

The morphology and nanostructure of the obtained Co_3O_4 and CuOeNiO/Co_3O_4 were evaluated by scanning electron microscopy. As shown in Fig. 3a and b, Co_3O_4 exhibits a platelike structure with a thickness of ca. 200 nm. It is also clearly shown that the Co_3O_4 plates are composed of small particles and the interspaces between these particles (as clearly presented in the SEM image in Fig. 3b) could provide more active sites available on the surface for catalytic reactions. After the CuOeNiO was deposited onto the surface of Co_3O_4 plates and heat-treated at 450 C, the obtained CuOeNiO/Co_3O_4 had a plate-like morphology with many smaller particles grown on the surface of these plates (Fig. 3c and d). Fig. 3d shows that these smaller CuOeNiO nanoparticles with an average size of ca. 200 nm were firmly anchored on these plates. The detailed structure of CuOeNiO/Co_3O_4 was further investigated by transmission electron microscopy (TEM). From Fig. 3e, it can be seen that the surface of CuOeNiO/Co_3O_4 is rough. Pores were also observed on the Co_3O_4 plate (Fig. 3f), indicating that porous Co_3O_4 was synthesized by this method. From Fig. 3f, it can be observed that the CuOeNiO nanoparticles formed on the Co_3O_4 plate are made up of smaller nanoparticles. Moreover, well-defined lattice fringes were found on the HR-TEM image of CuOeNiO particles. The *d*-spacing distance of these lattice fringes were measured to be 0.275 and 0.208 nm, corresponding to the (110) plane of CuO and (200) plane of NiO respectively. Other TEM images and selected area electron diffraction (SAED) pattern of CuOeNiO/Co_3O_4 nanoplate were shown in Fig. S1 in the supporting information. TEM image in Fig. S1a indicates that there are plenteous small nanoparticles on the surface of the nanoplate. These small nanoparticles aggregate together and form larger particles. This observation is in good agreement with SEM results. The characteristic diffraction cycles of CuO, NiO, and Co_3O_4 can be seen in Fig. S1b, indicative of a hybrid of CuO, NiO, and Co_3O_4.
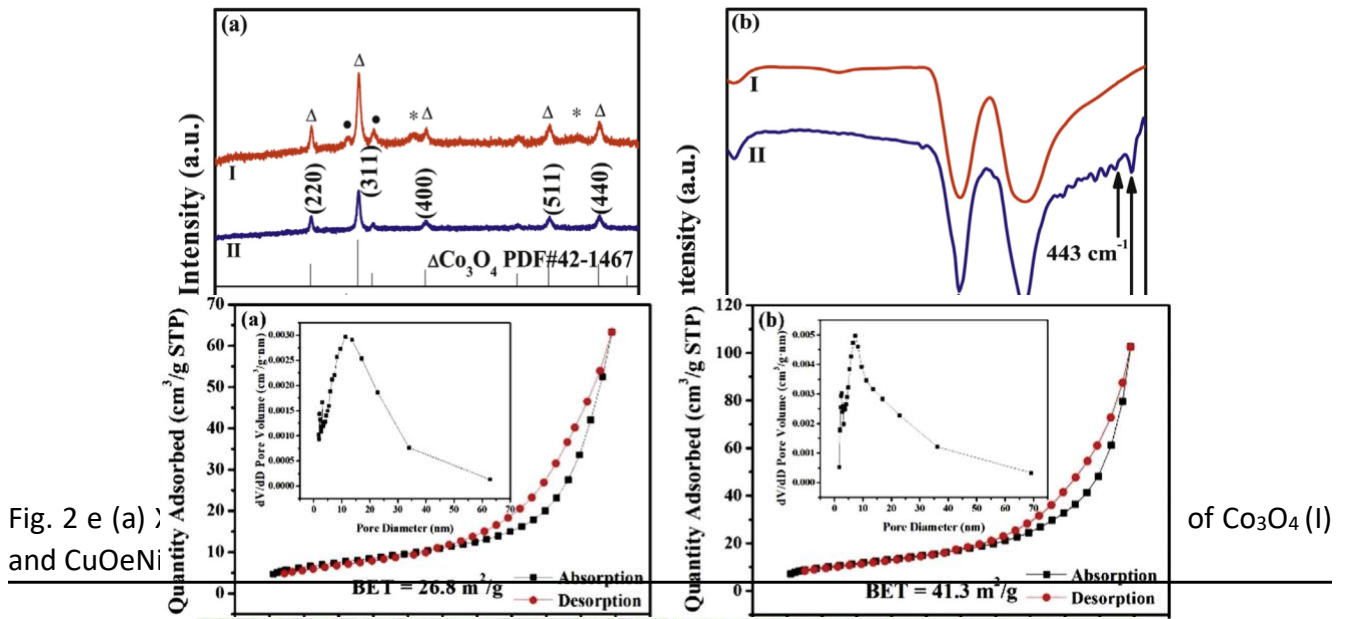
Fig. 2 e (a) X... of Co₃O₄ (I) and CuOeNi...
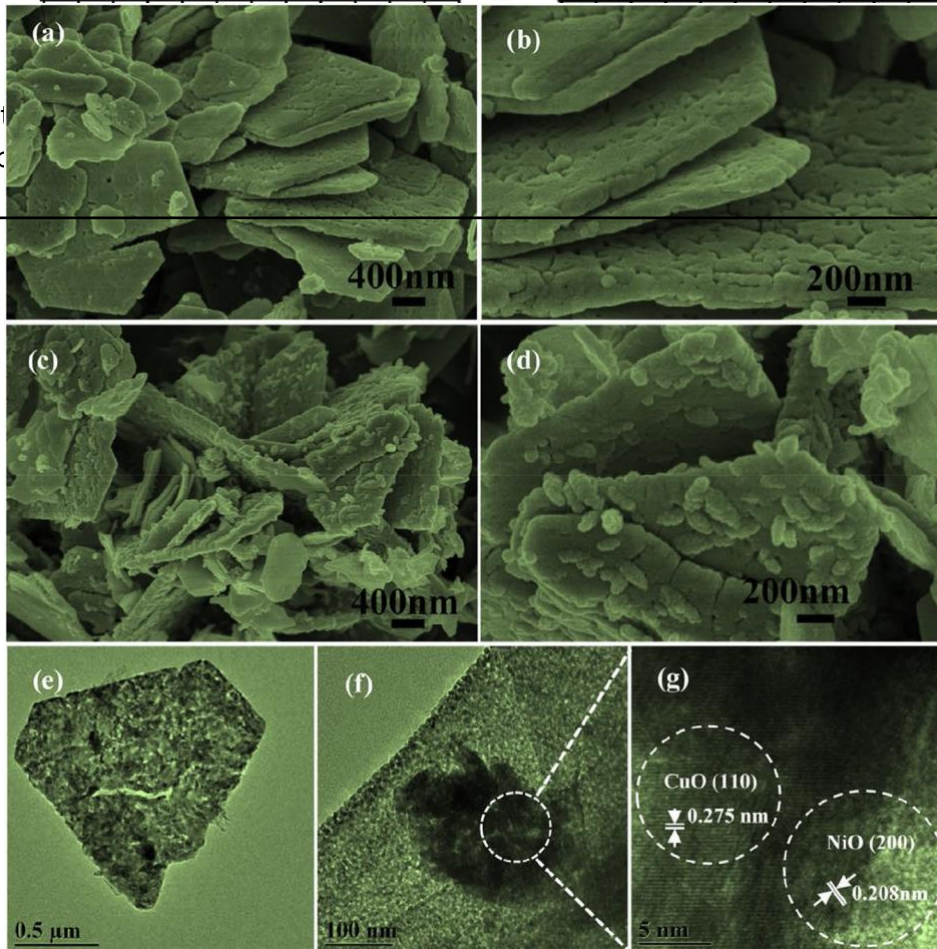
Fig. 4 e N₂ isot...)/Co₃O₄ hybrid nanoplates (b...

Fig. 3 e SEM images of Co₃O₄ nanoplates (a, b) and CuOeNiO/Co₃O₄ hybrid nanoplates (c, d); TEM images (e, f) of a piece of CuOeNiO/Co₃O₄ nanoplate and HRTEM image (g) taken on a particle on CuOeNiO/Co₃O₄ nanoplate.

N$_2$ isotherms adsorption-desorption were applied to investigate the porous structure of Co$_3$O$_4$ and CuOeNiO/Co$_3$O$_4$ (Fig. 4). Both samples exhibited a type II isotherm with a hysteresis loop at the relatively high-pressure region, suggesting that mesoporous structures existed in these two samples. The pore size distribution shown as the insets in Fig. 4 further confirms the presence of mesopores in Co$_3$O$_4$ and CuOeNiO/Co$_3$O$_4$. With the increase of relative pressure, the N$_2$ uptake of CuOeNiO/Co$_3$O$_4$ was clearly higher than that of Co$_3$O$_4$, indicating there were more pores formed on CuOeNiO/Co$_3$O$_4$ since CuOeNiO particles were made up of smaller particles and interspace between these small particles resulted in more pores available in the CuOeNiO/Co$_3$O$_4$ material. The BET surface areas of Co$_3$O$_4$ and CuOeNiO/Co$_3$O$_4$ were calculated to be 26.8 and 41.3 m^2 g^1 respectively.

The XPS analysis was applied to investigate the element states of CuOeNiO/Co$_3$O$_4$ (Fig. 5). The element signals of Cu 2p, Ni 2p, and Co 2p were detected on CuOeNiO/Co$_3$O$_4$ in its XPS survey spectrum (Fig. 4a). In the XPS spectra of Ni 2p (Fig. 4b), two doubles with satellite peaks were observed, attributing to Ni^{2b} 2$p_{3/2}$ (855.3 eV)/Ni^{2b} 2$p_{1/2}$ (873.2 eV) and Ni^{3b} 2$p_{3/2}$ (856.3 eV)/Ni^{3b} 2$p_{1/2}$ (874.8 eV) resulting from Ni^{2b} and Ni^{3b} bonded with oxygen [29]. Fig. 4c shows that there are two major peaks at ca. 954.2 and 934.4 eV with two satellite peaks corresponding to Cu 2$p_{1/2}$ and Cu 2$p_{3/2}$ respectively, indicating that the Cu in CuOeNiO/Co$_3$O$_4$ is in the form of Cu^{2b} [30]. In the deconvoluted high-resolution XSP spectrum of Co 2p, the peaks at 796.5 and 781.3 eV are attributed to Co^{2b}, and the other two peaks at 794.8 and 779.8 eV to Co^{3b} [31], namelyCo^{2b} and Co^{3b} co-existed in CuOeNiO/Co$_3$O$_4$.

The catalytic properties of these *as*-prepared samples were investigated by the hydrolysis of NH$_3$BH$_3$ in NaOH solution at 25 C in a thermostatic bath. Fig. 6a exhibits their corresponding hydrogen evolution curves. It should be mentioned that no hydrogen was produced without the catalyst, demonstrating that the catalyst is indispensable in this hydrolysis reaction. For all the three Co$_3$O$_4$,
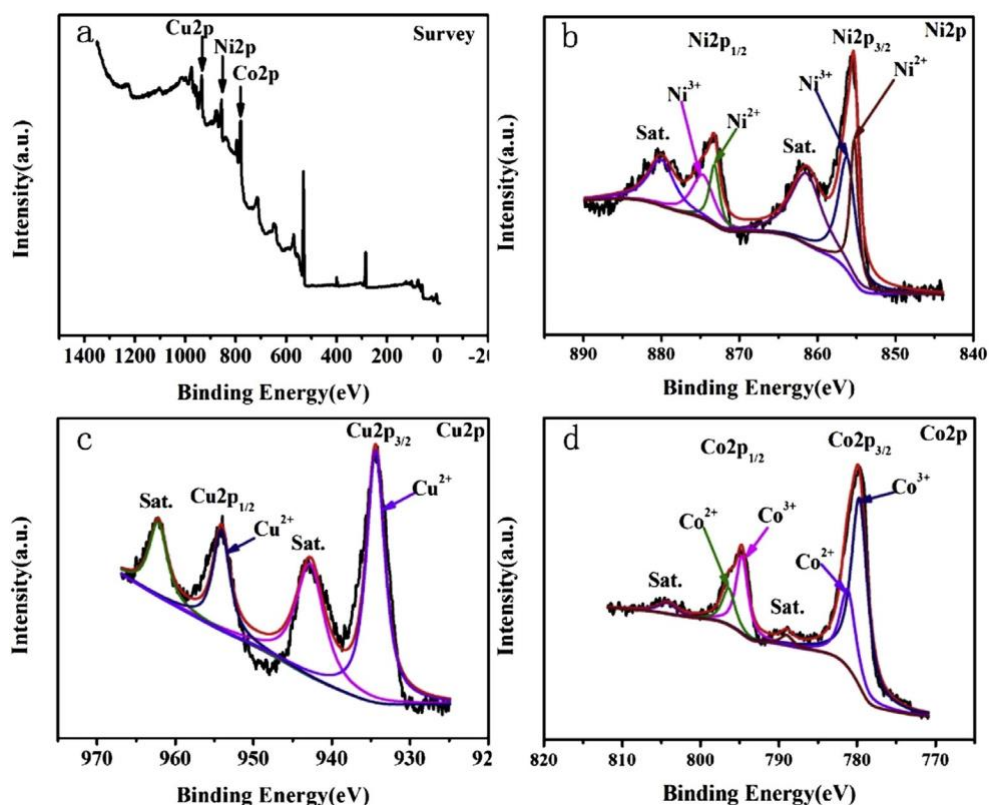

ig. 5 e XPS spectrum of survey scan of CuOeNiO/Co$_3$O$_4$ hybrid nanoplates (a), deconvoluted high-esolution XPS spectra of Ni 2p (b), Cu 2p (c) and Co 2p 3d (d) for CuOeNiO/Co$_3$O$_4$.

CuOeNiO, and CuOeNiO/Co$_3$O$_4$ samples, the molar ratio of H$_2$ and NH$_3$BH$_3$ can reach 3 (Fig. 6a), which is the theoretic ratio in case of complete hydrolysis of NH$_3$BH$_3$. This observation verifies that NH$_3$BH$_3$ can be completely hydrolyzed in the presence of them. Fig. 6a shows that CuO particles have very low activity towards the hydrolysis of NH$_3$BH$_3$ and the NiO particles are inert to the hydrolysis reaction. However, the CuO exhibited a very high catalytic activity when it was mixed with NiO, clearly demonstrating that the synergistic effect between CuO and NiO can significantly improve catalytic performance. Although Co$_3$O$_4$ is active towards the hydrolysis of NH$_3$BH$_3$, it takes about 100 s to activate this catalyst. It has been reported that the hydrolysis of NH$_3$BH$_3$ cannot be catalyzed by the Co^{2b} and Co^{3b} cations present in the catalyst, but metallic cobalt is active towards the NH$_3$BH$_3$ hydrolysis. When Co$_3$O$_4$ was mixed with NH$_3$BH$_3$ and NaOH in solution, it acted as a reducing agent in which cobalt cations were reduced to their metallic states yielding further NH$_3$BH$_3$ hydrolysis. Since the Co cations have relatively high standard reduction potential, (E^{ϕ} (Co^{2b}/Co) ¼0.280 V vs. SHE), Co^{2b} was not easily reduced [32]. This could explain the reason for an activating period for Co$_3$O$_4$. Although CuO is a low catalytically active material towards the hydrolysis, no activating period was observed, since Cu^{2b} was easily reduced to its metallic state due to its relatively high reduction potential (E^{ϕ} (Cu^{2b}/Cu) ¼ 0.337 vs. SHE) [32]. When the active Co$_3$O$_4$ was integrated into the CuOeNiO matrix, the synergistic effect between these three metal oxides exhibited a very high catalytic activity towards the NH$_3$BH$_3$ hydrolysis, and the NH$_3$BH$_3$ could be completely hydrolyzed in just 160 s. The catalytic performance of the materials was also quantified by the turnover frequency (TOF) value as shown in Fig. 6b. From the figure, it can be observed that the TOF of CuOeNiO/Co$_3$O$_4$ (79.1 mol$_{H2}$ mol cat^1 min^1) had almost a 4-fold higher value than that of CuOeNiO and Co$_3$O$_4$, which further indicated that the synergistic effect played a significant role in enhancing the catalytic performance.

To shed some light on the NH$_3$BH$_3$ hydrolysis process on these catalysts, H$_2$-TPR analysis was carried out and the results are presented in Fig. 7. In the case of Co$_3$O$_4$, two prominent H$_2$ consumption peaks at 270.5 and 325.2 C, attributed to the reactions of Co$_3$O$_4$ to CoO and CoO to Co respectively, can be observed [33]. For NiO, two main reduction peaks are found at 265.6 and 313.7 C and can be ascribed to the reduction of Ni^{2b} to Ni^{db} and the reaction of Ni^{db} to Ni respectively [34]. In the H$_2$-TPR curve of CuO, only one reduction peak can be observed at 235.2 C, due to the reduction of Cu^{2b} [35]. When three of these metal oxides were combined together, the reduction peaks of CuOeNiO/Co$_3$O$_4$ shifted to lower temperatures, indicating that the reduction reactions became much easier due to the synergistic effect between CuO, NiO, and Co$_3$O$_4$.

It has been reported that the metallic Cu can be fastly and easily formed on the surface of Co$_3$O$_4$ and then the formed Cu could act as the active sites to accelerate the reduction of cobalt cations. The newly formed metallic Co nanoparticles were found to be catalytically active towards the hydrolysis of NH$_3$BH$_3$. It was also found that by introducing NiO into CuO to form CuOeNiO hybrid can efficiently improve the catalytic activity of CuO due to the synergetic interaction between Cu and Ni [36]. After the CuOeNiO/Co$_3$O$_4$ was mixed with NH$_3$BH$_3$, the element states of CuOeNiO/Co$_3$O$_4$ were further evaluated by XPS analysis. As shown in Fig. 8, it is clearly shown that metallic Ni, Cu, and Co were formed on the CuOeNiO/Co$_3$O$_4$ after it was used to catalyze the hydrolysis of NH$_3$BH$_3$, and their synergistic interaction could significantly improve the catalytic activity.
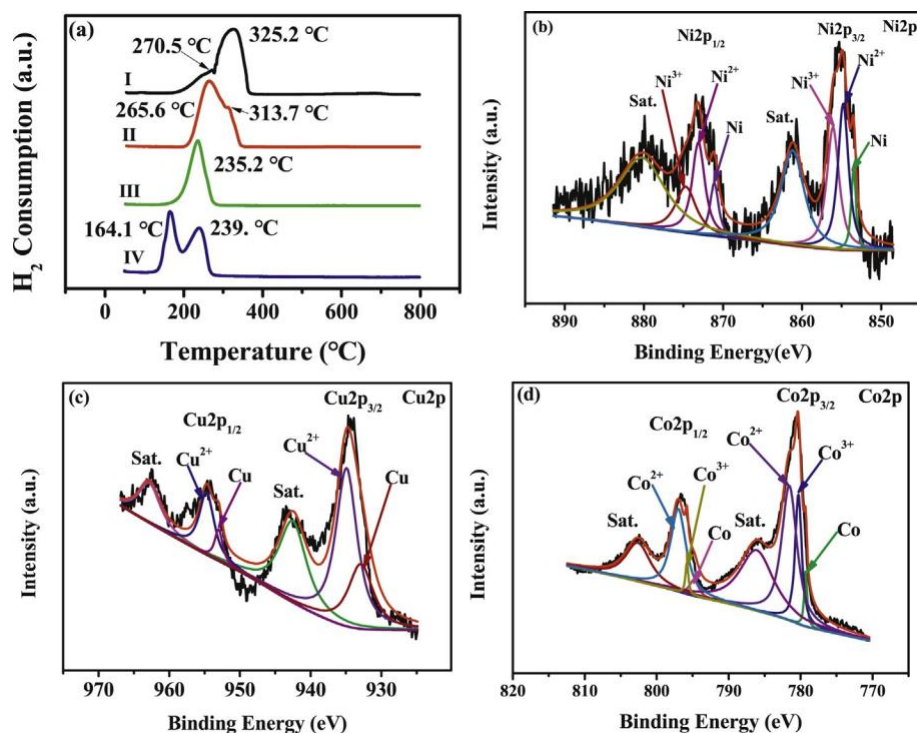
For comparison, Table 1 displays the TOF of other noblemetal-free catalysts reported in the literature recently, as well as that of the as-prepared CuOeNiO/Co₃O₄ catalysts. Evidently, the CuOeNiO/Co₃O₄ hybrid nanoplate is one of the most active catalysts towards NH₃BH₃ hydrolysis in terms of TOF.

The effect of different NH₃BH₃ concentrations on the hydrogen generation rates was carried out to investigate the NH₃BH₃ hydrolysis kinetics. The hydrogen generation values *versus* time on CuOeNiO/Co₃O₄ in various NH₃BH₃ concentrations, and their hydrogen generation rates *versus* NH₃BH₃ concentration in natural logarithmic scale are shown in Fig. 8a and b respectively. The slope of *ln*(rate) *vs*. *ln*(AB) was found to be 0.15, indicating that the NH₃BH₃ hydrolysis occurring on CuOeNiO/Co₃O₄ was a zero-order reaction with respect to NH₃BH₃ concentration. This finding also infers that the NH₃BH₃ was easily activated on CuOeNiO/Co₃O₄. It was also reported that the hydrolysis reaction was significantly
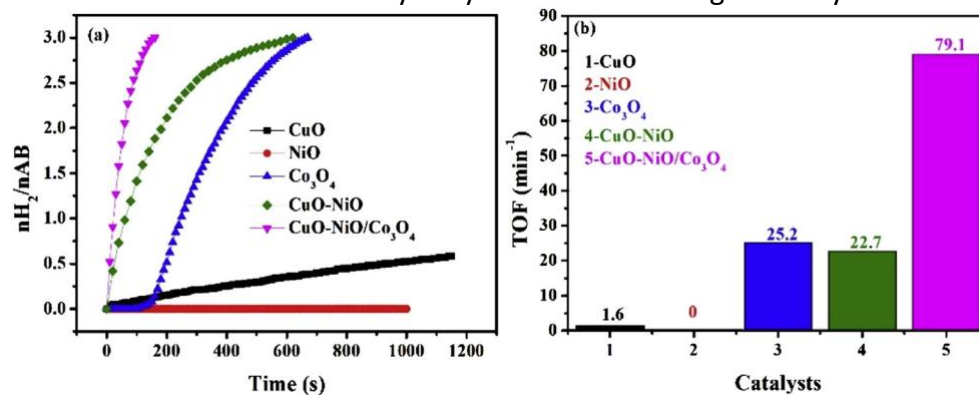

Fig. 6 e Plots of molar ratio of hydrogen to NH₃BH₃ versus time for CuO, NiO, Co₃O₄, CuOeNiO and CuOeNiO/Co₃O₄ samples (a) and their corresponding TOF (b).

Fig. 7 e (a) H₂-TPR curves of Co₃O₄ (I), NiO (II); CuO (III) and CuOeNiO/Co₃O₄ (Ⅳ); Deconvoluted high-resolution XPS spectra of Ni 2p (b), Cu 2p (c) and Co 2p (d) on CuOeNiO/Co₃O₄ after the hydrolysis test.
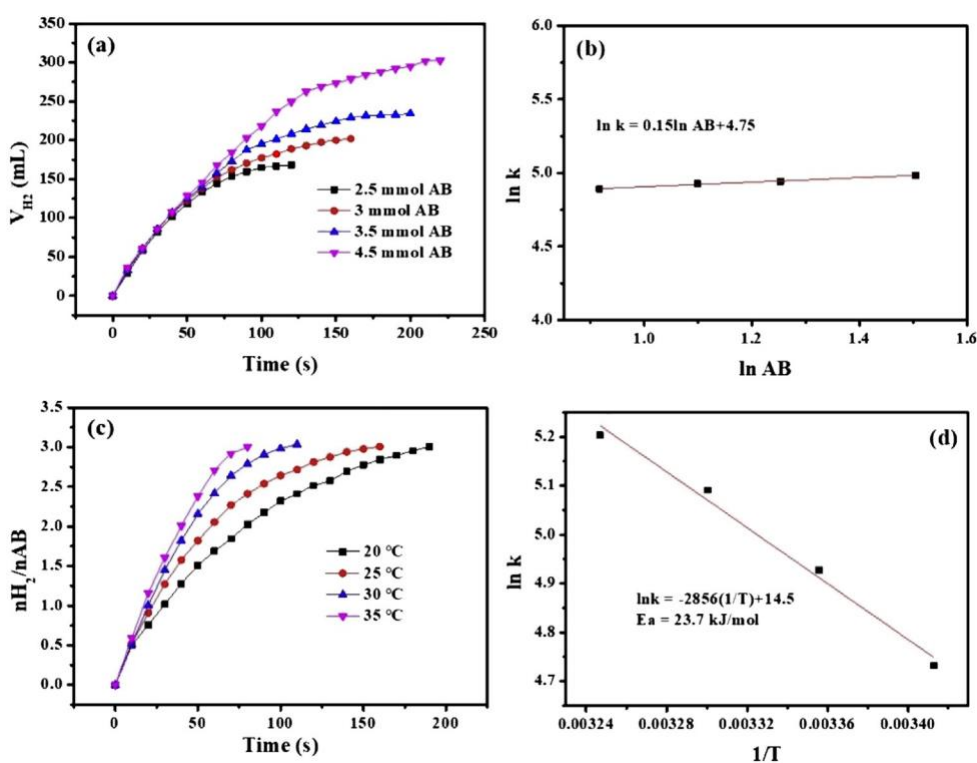
Fig. 8 e The effect of concentration of NH_3BH_3 on the hydrogen generation rates (a); and plot of ln(hydrogen generation rate) vs. ln(NH_3BH_3 concentration) (b); the effect of temperature on hydrolysis of NH_3BH_3 on CuOeNiO/Co₃O₄ (c); and the Arrhenius plot of NH_3BH_3 hydrolysis rates (d).

Catalysts	TOF/molHydrogen$molcat.1 $min1	Ref
CoxCu1xCo2O4@CoyCu1yCo2O4 yolkeshell microspheres	81.8	[26]
Cu0.5Co0.5O-rGO	81.7	[21]
CuOeNiO/Co₃O₄	79.1	This work
Cu$_x$Co$_{1-x}$O/Graphene Oxide	70.0	[8]
Cu(OH)₂/Fe(OH)₃	50.3	[24]
CuCo₂O₄ film	44.0	[37]
CoCu/Ni foam	30.5	[38]
MoO₃-doped MnCo₂O₄ 26.4 [39] CuNi/MIL-101	20.9 [17] Graphene-CuCo 9.18	
[22]		
Co@NeC-700	5.6	[40]

affected by temperature [3]. Therefore, the effect of temperature on the hydrogen generation rates was also investigated on CuOeNiO/Co₃O₄ at several temperatures in the range of 20e35 C (Fig. 8c and d). As shown in Fig. 8c, the amount of generated hydrogen increased rapidly with temperature. The apparent activation energy (E_a) was measured by using the *Arrhenius* equation, namely ln k ¼ $RT\frac{Ea}{}$þ ln$A$, where k is the rate constant (s1) of the hydrolysis reaction, E_a is the activation energy (kJ mol1), R the molar gas constant (8.31 kJ mol1 K1) and T the reaction temperature (K). As shown in Fig. 8d, the Ea of NH₃BH₃ hydrolysis on CuOeNiO/ Co₃O₄ was calculated to be 23.7 kJ mol1. The reusability of the CuOeNiO/Co₃O₄ hybrid catalyst was also evaluated and the resultsweredisplayedin Fig.S2. It wasfound that thecatalytic activity of the catalyst slightly decrease with the cycle number. However, the molar ratio of hydrogen to ammonia borane was still 3 even at the 5th cycle, verifying that the complete hydrogen release could be achieved, implying that the CuOeNiO/Co₃O₄ catalyst possesses relatively high stability and good reusability.

Conclusions

In summary, CuOeNiO/Co₃O₄ hybrid with plate-like morphology was successfully synthesized through a simple hydrothermal method. The *as-prepared* CuOeNiO/Co₃O₄ hybrid of the mesoporous structure was made up of irregular small porous nanoparticles with rough and rich particle boundaries. It was found that by introducing NiO into the hybrid could efficiently improve the catalytic activity, and the presence of CuO could significantly reduce the activating period. There was a synergistic effect between CuO and NiO, CuOeNiO and Co₃O₄ in NH₃BH₃ hydrolysis. The H₂-TPR results gave a hint that the reducibility of the catalysts played an important role in determining their catalytic activity. When the CuOeNiO/Co₃O₄ hybrid material was used as a catalyst for the hydrolysis of NH₃BH₃, it exhibited a good catalytic activity with a TOF value of 79.1 mol$_{H2}$ mol cat1 min1. Our findings also suggested that the *as-prepared* CuOeNiO/Co₃O₄ hybrid material could be a promising material in producing hydrogen by using NH₃BH₃ as hydrogen-rich material for practical applications.

R E F E R E N C E S

---

[1] Schlapbach L, Zu¨ttel A. Hydrogen-storage materials for mobile applications. Mater Sustain Energy 2010:265e70.

[2] Ding J, Ji S, Wang H, Key J, Dan JLB, Wang R. Nano-engineered intrapores in nanoparticles of PtNi networks for increased oxygen reduction reaction activity. J Power Sources 2018;374:48e54.

[3] Wang X, Liao J, Li H, Wang H, Wang R, Pollet BG, et al. Highly active porous CoeB nanoalloy synthesized on liquid-gas interface for hydrolysis of sodium borohydride. Int J Hydrogen Energy 2018;43:17543e55.

[4] Masjedi-Arani M, Salavati-Niasari M. Facile precipitation synthesis and electrochemical evaluation of Zn2SnO4 nanostructure as a hydrogen storage material. J Hydrogen Energy 2017;42:12420e9.

[5] Salehabadi A, Salavati-Niasari M, Gholami T. Green and facial combustion synthesis of Sr₃Al₂O₆ nanostructures; a potential electrochemical hydrogen storage material. J Clean Prod 2018;171:1e9.

[6] Gholami T, Salavati-Niasari M, Varshoy S. Electrochemical hydrogen storage capacity and optical properties of NiAl2O4/ NiO nanocomposite synthesized by green method. Int J Hydrogen Energy 2017;42:5235e45.

[7] Gholami T, Salavati-Niasari M, Varshoy S. Investigation of electrochemical hydrogen storage and photocatalytic properties of CoAl2O4 pigment: green synthesis and characterization. Int J Hydrogen Energy 2016:9418e26.

[8] Feng K, Zhong J, Zhao B, Zhang H, Xu L, Sun X, et al. Cux Co1x O nanoparticles on graphene oxide as A synergistic catalyst for high-efficiency hydrolysis of ammonia-borane. Angew Chem 2016;55:11950e4.

[9] Ekinci A, S,ahin O, Saka C, Avci T. The effects of plasm€ a treatment on electrochemical activity of CoeWeB catalyst for hydrogen production by hydrolysis of NaBH4. Int J Hydrogen Energy 2013;38:15295e301.

[10] Yao Q, Yang K, Nie W, Li Y, Lu Z-H. Highly efficient hydrogen generation from hydrazine borane via a MoOx-promoted NiPd nanocatalyst. Renew Energy 2020;147:2024e31.

[11] Bekirogullari M, Kaya M, Saka C. Highly efficient Co-B catalysts with chlorella vulgaris microalgal strain modified using hydrochiric acid as a new support material for hydrogen production from methanolysis of sodium borohydride. Int J Hydrogen Energy 2019;44:7262e75.

[12] Balbay A, Saka C. The effect of the concentration of hydrochloric acid and acetic acid aqueous solution for fast hydrogen

production from methanol solution of NaBH4. Int J Hydrogen Energy 2018;43:14265e72.

[13] Sait Izgi M, S,ahin O, Saka C€ . g-Al2O3 supported/Co-Cr-B catalyst for hydrogen evolution via NH3BH3 hydrolysis. Mater Manuf Process 2019;34:1620e6.

[14] Xu D, Zhang H, Ye W. Hydrogen generation from hydrolysis of alkaline sodium borohydride solution using Pt/C catalyst. Catal Commun 2007;8:1767e71.

[15] Kec¸eli E, Ozkar S. Ruthenium(III) acetylacetonate:€ a homogeneous catalyst in the hydrolysis of sodium borohydride. J Mol Catal A Chem 2008;286:87e91.

[16] Patel N, Patton B, Zanchetta C, Fernandes R, Guella G, Kale A, et al. Pd-C powder and thin film catalysts for hydrogen production by hydrolysis of sodium borohydride. Int J Hydrogen Energy 2008;33:287e92.

[17] Gao D, Zhang Y, Zhou L, Yang K. CuNi NPs supported on MIL101 as highly active catalysts for the hydrolysis of ammonia borane. Appl Surf Sci 2018;427:114e22.

[18] Wang H, Zhou L, Han M, Tao Z, Cheng F, Chen J. CuCo nanoparticles supported on hierarchically porous carbon as catalysts for hydrolysis of ammonia borane. J Alloys Compd 2015;651:382e8.

[19] Li C, Wang D, Wang Y, Li G, Hu G, Wu S, et al. Enhanced catalytic activity of the nanostructured Co-W-B film catalysts for hydrogen evolution from the hydrolysis of ammonia borane. J Colloid Interface Sci 2018;524:25e31.

[20] Hou C-C, Li Q, Wang C-J, Peng C-Y, Chen Q-Q, Ye H-F, et al. Ternary NieCoeP nanoparticles as noble-metal-free catalysts to boost the hydrolytic dehydrogenation of ammonia-borane. Energy Environ Sci 2017;10:1770e6.

[21] Zheng H, Feng K, Shang Y, Kang Z, Sun X, Zhong J. Cube-like CuCoO nanostructures on reduced graphene oxide for H2 generation from ammonia borane. Inorg Chem Front 2018;5:1180e7.

[22] Yan J-M, Wang Z-L, Wang H-L, Jiang Q. Rapid and energyefficient synthesis of a grapheneeCuCo hybrid as a high performance catalyst. J Mater Chem 2012;22:10990.

[23] Yamada Y, Yano K, Xu Q, Fukuzumi S. Cu/Co3O4 nanoparticles as catalysts for hydrogen evolution from ammonia borane by hydrolysis. J Phys Chem C 2010;114:16456e62.

[24] Peng C-Y, Hou C-C, Chen Q-Q, Wang C-J, Lv X-J, Zhong J, Fu W-F, Chi C-M, Chen Y. Cu(OH)2 supported on Fe(OH)3 as a synergistic and highly efficient system for the dehydrogenation of ammonia-borane. Sci Bull 2018;63:1583e90.

[25] Lu Z-H, Li J, Feng G, Yao Q, Zhang F, Zhou R, et al. Synergistic catalysis of MCM-41 immobilized CueNi nanoparticles in hydrolytic dehydrogeneration of ammonia borane. Int J Hydrogen Energy 2014;39:13389e95.

[26] Lu D, Li J, Lin C, Liao J, Feng Y, Ding Z, et al. A simple and scalable route to synthesize CoxCu1xCo2O4@CoyCu1yCo2O4 yolkeshell microspheres, A high-performance catalyst to hydrolyze ammonia borane for hydrogen production. Small 2019;15:1805460.

[27] Davar F, Fereshteh Z, Salavati-Niasari M. Nanoparticles Ni and NiO: synthesis, characterization and magnetic properties. J Alloys Compd 2009;476:797e801.

[28] El-Sayed AM, Ismail FM, Yakout SM. Synthesis and structural investigations of Ag-added BaTiO3-CuO mixed oxide for CO2 gas sensing. Int J Chem Eng 2011;2011.

[29] Wu D, Ming W, Lin X, Wu Q, Chen H. A NiCo/NiOeCoOx
ultrathin layered catalyst with strong basic sites for highperformance H2 generation from hydrous hydrazine. J Mater Chem A 2016;4:6595e602.

[30] He G, Qiao M, Li W, Lu Y, Zhao T, Zou R, et al. N-Co-Doped graphene-nickel cobalt sulfide aerogel: improved energy storage and electrocatalytic performance. Adv Sci 2017;4 [n/a-n/a].

[31] Cui J, Zhang X, Tong L, Luo J, Wang Y, Zhang Y, et al. A facile synthesis of mesoporous Co3O4/CeO2 hybrid nanowire arrays for high performance supercapacitors. J Mater Chem A 2015;3:10425e31.

[32] Li C, Zhou J, Gao W, Zhao J, Liu J, Zhao Y, et al. Binary CueCo catalysts derived from hydrotalcites with excellent activity and recyclability towards NH3BH3 dehydrogenation. J Mater Chem A 2013;1:5370.

[33] Bulavchenko OA, Gerasimov EY, Afonasenko TN. Reduction of double manganeseecobalt oxides: in situ XRD and TPR study. Dalton Trans 2018;47:17153e9.

[34] Du X, Yao T-L, Wei Q, Zhang H, Huang Y. Investigation of FeNi mixed-oxide catalysts for the reduction of NO by CO: physicochemical properties and catalytic performance. Chem Asian J 2019;14:2966e78.

[35] Song S, Jiang S. Selective catalytic oxidation of ammonia to nitrogen over CuO/CNTs: the promoting effect of the defects of CNTs on the catalytic activity and selectivity. Appl Catal B Environ 2012;117e118:346e50.

[36] Yen H, Kleitz F. High-performance solid catalysts for H2 generation from ammonia borane: progress through synergetic CueNi interactions. J Mater Chem A 2013;1:14790e6.

[37] Liu Q, Zhang S, Liao J, Feng K, Zheng Y, Pollet BG, Li H. CuCo2O4 nanoplate film as a low-cost, highly active and durable catalyse towards the hydrolytic dehydrogenation of ammonia borane for hydrogen production. J Power Sources 2017;355:191e8.

[38] Liao J, Lv F, Feng Y, Zhong S, Wu X, Zhang X, Wang H, Li J, Li H. Electromagnetic-field-assisted synthesis of Ni foam film-supported CoCu alloy microspheres composed of nanosheets: a high performance catalyst for the hydrolysis of ammonia borane. Catal Commun 2019;122:16e9.

[39] Lu D, Feng Y, Ding Z, Liao J, Zhang X, Liu H-R, Li H. MoO₃Doped MnCo₂O₄ microspheres consisting of nanosheets: an inexpensive nanostructured catalyst to hydrolyze ammonia borane for hydrogen generation. Nanomaterials 2019;9:1e9.

[40] Wang H, Zhao Y, Cheng F, Tao Z, Chen J. Cobalt nanoparticles embedded in porous N-doped carbon as longlife catalysts for hydrolysis of ammonia borane. Catal Sci Technol 2016;6:3443e8.